Supporting Information

Monitoring Plant Health with Near Infrared Fluorescent H_2O_2 Nanosensors

Honghong Wu[1,2+], Robert Nißler[3+], Victoria Morris[1], Niklas Herrmann[3], Peiguang Hu[1], Su-Ji Jeon[1], Sebastian Kruss[3]*, Juan Pablo Giraldo[1]*

[1], Department of Botany and Plant Sciences, University of California, Riverside, CA, USA, 92521
[2], College of Plant Science & Technology, Huazhong Agricultural University, Wuhan, China, 430070
[3], Institute of Physical Chemistry, Georg August University Göttingen, Göttingen, Germany, 37077

+ These authors contributed equally to this paper.
* Corresponding authors: juanpablo.giraldo@ucr.edu, skruss@uni-goettingen.de

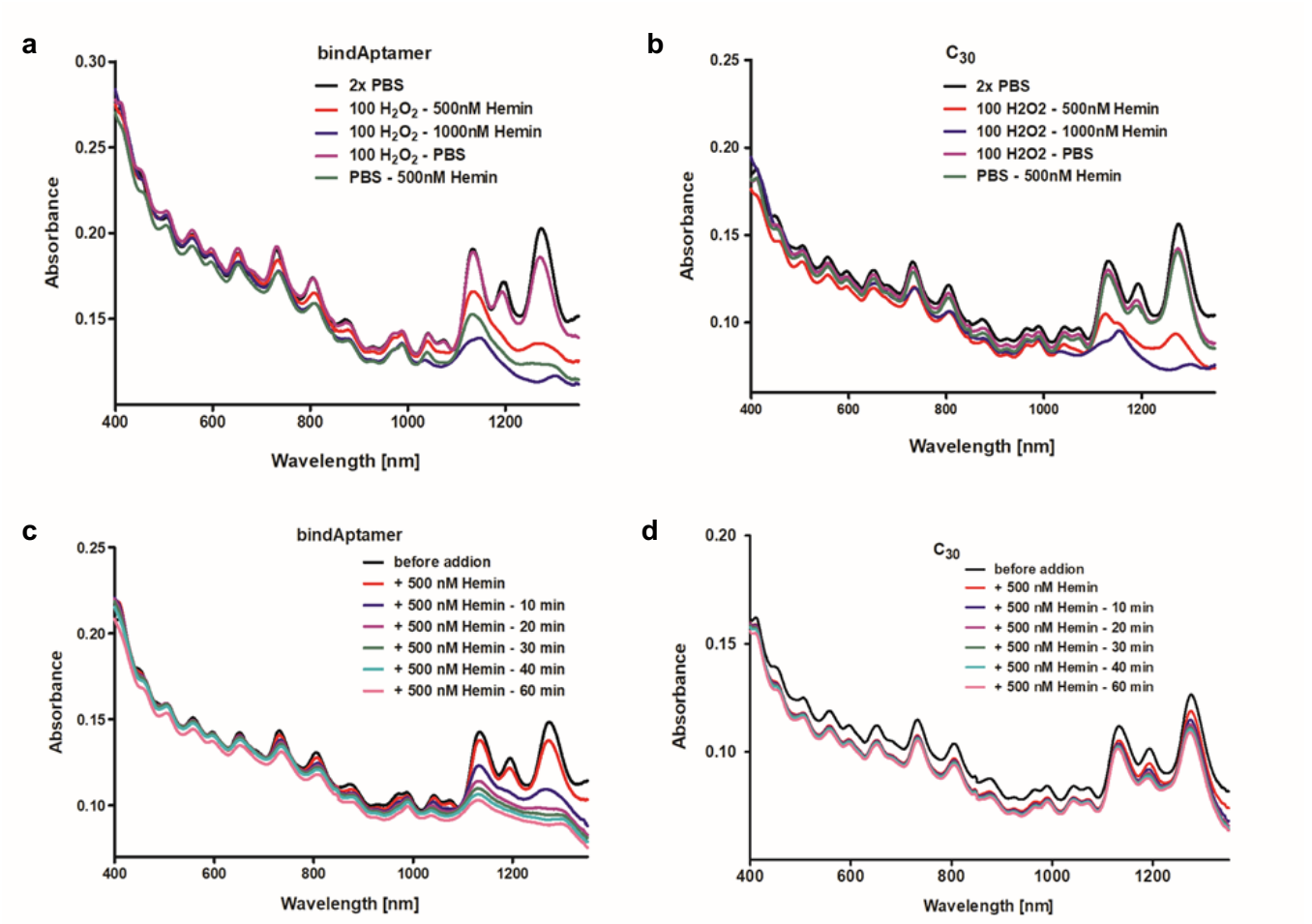

Figure S1 | Absorbance spectra of larger diameter (HiPco) SWCNTs in the presence of hemin and H_2O_2. a, HeAptDNA-HiPco-SWCNTs after 24 h incubation with varying hemin concentrations and 100 µM H_2O_2. The decrease of absorbance features of larger SWCNT chiralites is more prominent when using HiPco (Nano Integris HiPco Raw SWCNTs) samples. **b,** Complementary experiment with C_{30}–HiPco-SWCNTs shows a similar effect on larger chiralities upon exposure to H_2O_2 and hemin, but not after solely hemin addition. **c,** Absorbance spectra of HeAptDNA-HiPco-SWCNTs after addition of 500 nM Hemin. A strong reduction during the first 10 min is detectable and increases during the timeframe of the experiment. This shows that the binding of hemin to larger SWCNT chiralites affects their photophysics and stability, which makes them less suitable for H_2O_2 sensing. **d,** C_{30}–HiPco-SWCNTs having no binding affinity to hemin show no reduction of absorbance features.

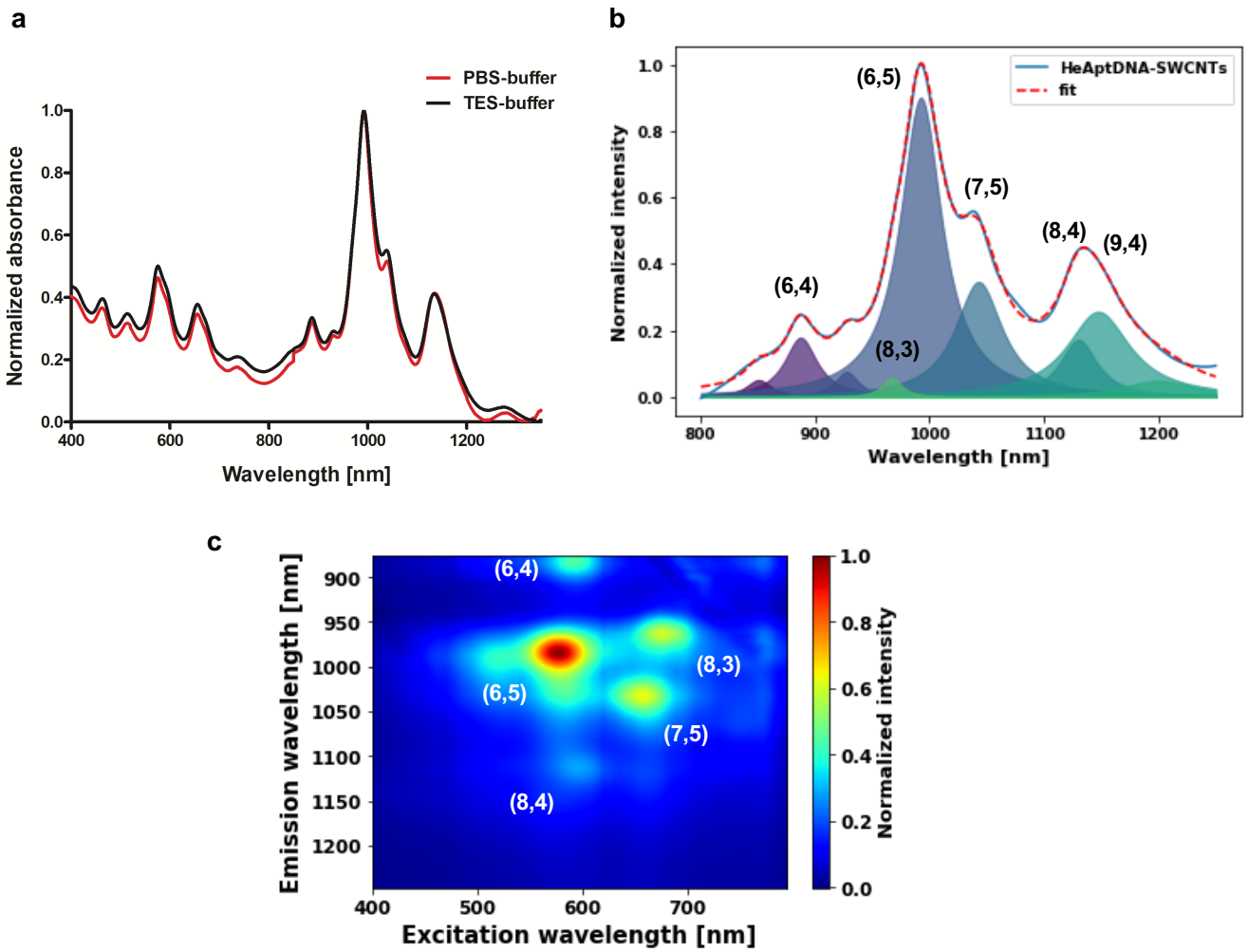

Figure S2 | Optical characterization of HeAptDNA-SWCNT. a, The distinct absorption features of (6,5)-enriched SWCNTs indicate well-dispersed SWCNTs with a maximum peak at 992.4 nm for (6,5)-SWCNTs, both in PBS and TES buffer. **b,** Fitted absorption of E_{11} transitions of the HeAptDNA-SWCNTs show minor chirality fractions of (6,4), (8,3), (7,5), (8,4), and (9,4) SWCNTs. **c,** 2D excitation-emission spectra of HeAptDNA-SWCNTs indicate the most prominent nIR emission from the (6,5) chirality, followed by (7,5), (8,3), and (6,4)-SWCNT chiralities with lower nIR intensity.

Figure S3

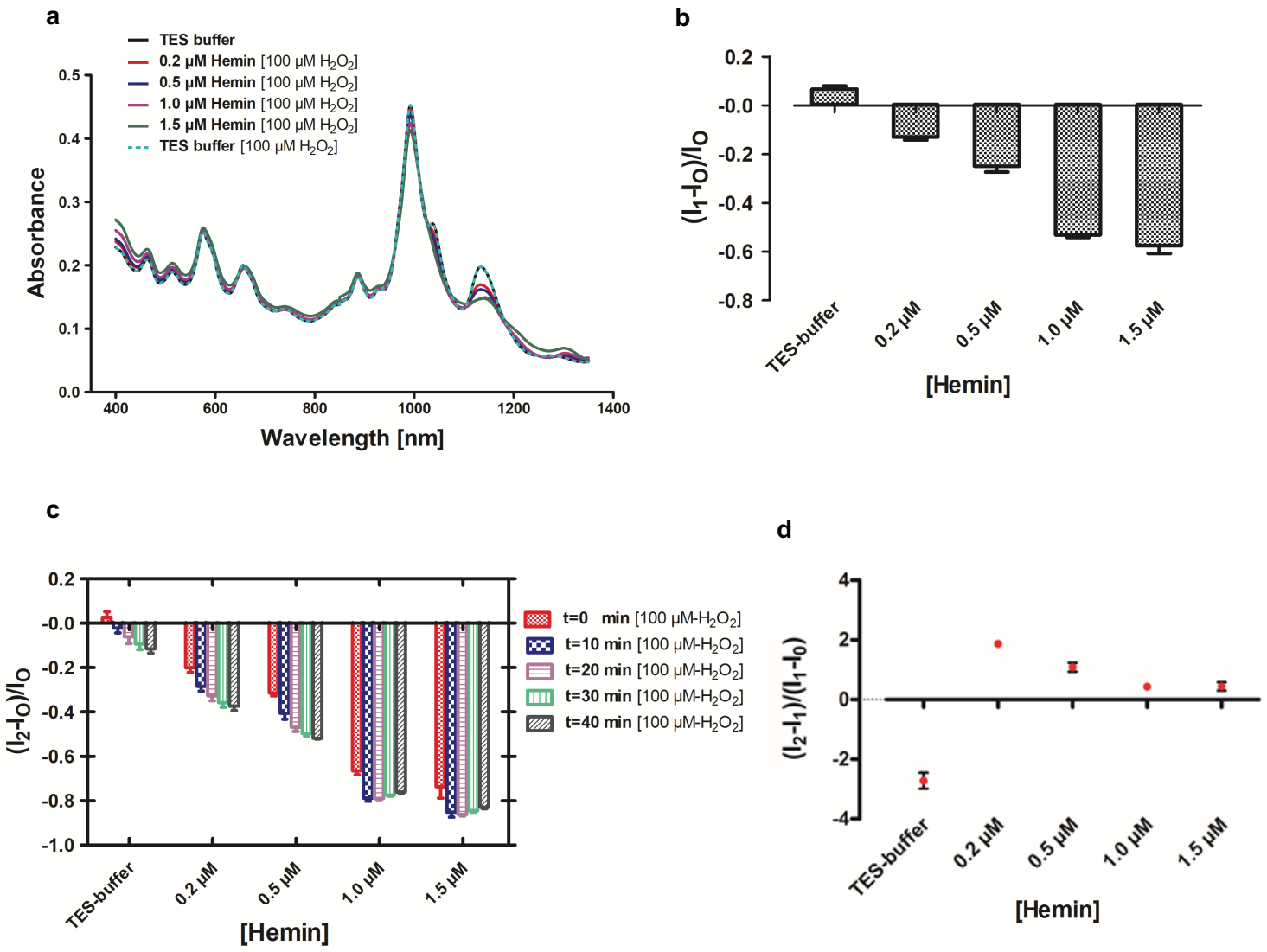

Figure S3 | Advanced *in vitro* characterization of HeAptDNA-SWCNT based H_2O_2 sensors. a, Absorbance spectra of HeAptDNA-SWCNTs having different hemin concentrations in response to 100 μM H_2O_2. The absorbance of some larger SWCNT chiralites (> 1100 nm) slightly decreases in the presence of hemin and H_2O_2 while (6,5)-SWNCTs features are preserved, indicating high stability. **b,** Fluorescence response of 2 nM HeAptDNA-(6,5)-SWCNTs to different hemin concentrations (n=3, error = SD). A higher hemin concentration leads to a stronger SWCNT fluorescence reduction which can hamper *in vivo* imaging in plant tissue due to low fluorescence signal. **c,** Fluorescence response of 2 nM HeAptDNA-SWCNTs with different hemin concentrations to 100 μM H_2O_2. The $(I_2\text{-Io})/\text{Io}$ is a relative value comparing the initial fluorescence emission (Io) with quenching events due to both hemin and H_2O_2 addition (I_2) (n=3, error = SD). **d,** Ratio between the hemin (I_1) and H_2O_2 (I_2) quenching events $(I_2\text{-}I_1)/(I_1\text{-}I_0)$ reveals that concentrations between 0.2 and 0.5 μM hemin are best suitable for H_2O_2 sensing (n=3, error = SD).

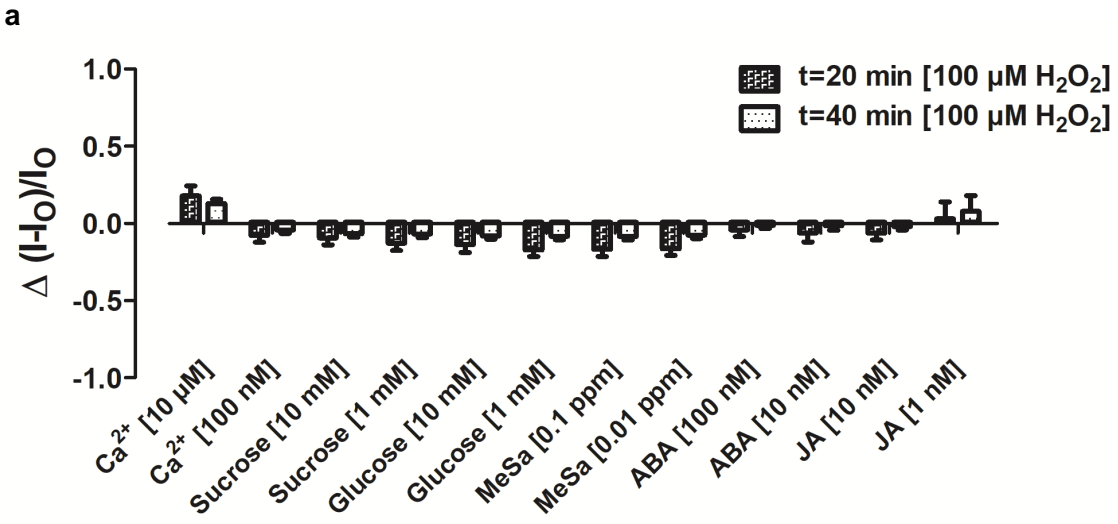

Figure S4 | Assessment of the influence of plant stress induced metabolites on H_2O_2 sensing performance of HeAptDNA-SWCNT. The Δ $(I-I_0)/I_0$ describes the difference in nIR emission intensity response to H_2O_2 between HeAptDNA-SWCNTs (2 nM) in TES-buffer and in the presence of plant metabolites associated with stress (Ca^{2+}, sucrose, glucose, MeSa - Methyl salicylate, ABA - Abscisic acid, JA - Jasmonic acid). A positive Δ $(I-I_0)/I_0$ can be interpreted as a reduction in sensor fluorescence response whereas a negative Δ $(I-I_0)/I_0$ indicates a stronger fluorescence response to H_2O_2 sensing. The effect of plant metabolites during H_2O_2 sensing is less prominent after 40 min (n=3; error = SD).

Figure S5

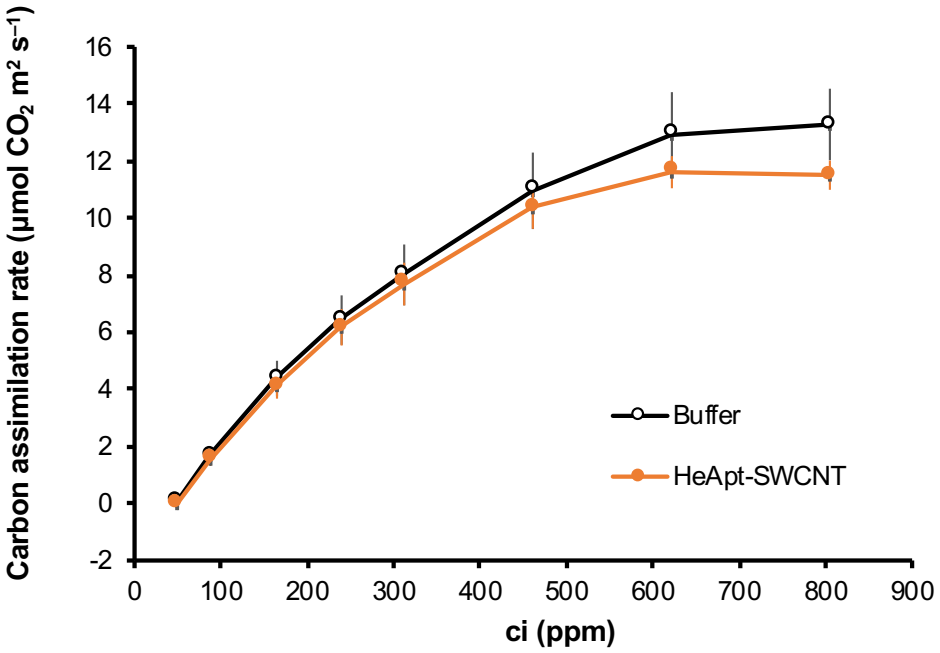

Figure S5 | No impact of HeAptDNA-SWCNT sensors on plant photosynthesis. Carbon assimilation rates under varied internal CO_2 concentrations (ci) in leaves infused with buffer (control) or HeAptDNA-SWCNT. No statistical differences in carbon assimilation rates were observed between controls and nanosensor treated plants at each CO_2 level ($p < 0.05$, Student's t-test). Mean ± SE (n = 6).

Figure S6

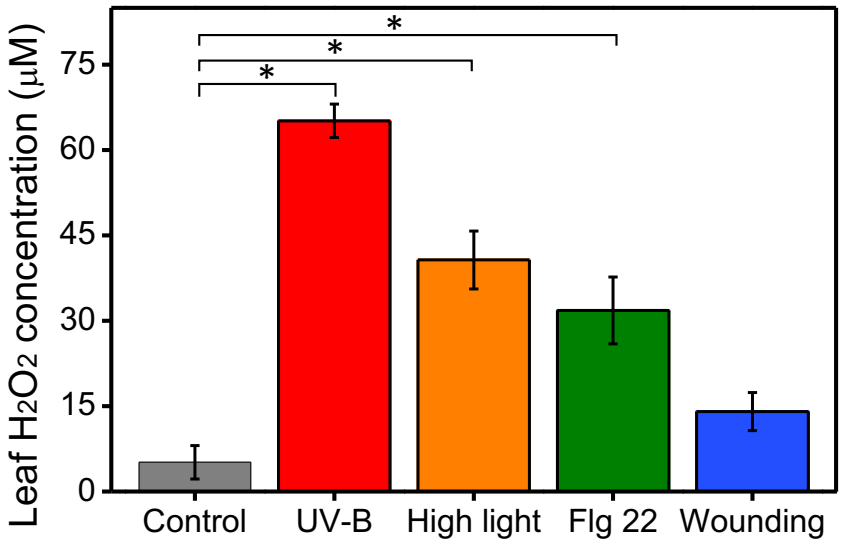

Figure S6 | Leaf H_2O_2 content in leaves of plants under stress. Determination of H_2O_2 concentration in leaves by a quantitative peroxide assay from plants exposed to UV-B light (365 nm, 90 min), high light (1800 μmol m^{-2} s^{-1} of photosynthetic active radiation, 90 min), flg 22 peptide (10 μM, 60 min), leaf wounding, and no stress (controls). Significant differences in leaf H_2O_2 content were observed between control leaves and UV-B light, high light, and flg 22 but not compared to leaf wounding ($p < 0.05$, Student's t-test). Mean ± SE (n = 3).